p-leader based classification of first stage intrapartum fetal HRV

Roberto Leonarduzzi, Jiri Spilka, Herwig Wendt, Stéphane Jaffard, Maria E. Torres, Patrice Abry, Muriel Doret

p-leader based classification of first stage intrapartum fetal HRV

R. F. Leonarduzzi[1], J. Spilka[2], H. Wendt[3], S. Jaffard[4], M. E. Torres[1], P. Abry[2] and M. Doret[5]

[1] CONICET and LSDNL, Universidad Nacional de Entre Ríos, Argentina,`rleonarduzzi@bioingenieria.edu.ar`
[2] CNRS, Physics Department, ENS de Lyon, France, `patrice.abry@ens-lyon.fr`
[3] IRIT - ENSEEIHT, CNRS, University of Toulouse, France, `herwig.wendt@irit.fr`
[4] LAMA, Math. Dept., Université Paris-Est Creteil (UPEC), Créteil, France, `stephane.jaffard@u-pec.fr`
[5] Hospices Civil de Lyon Femme-Mère-Enfant Hospital, Lyon, France, `muriel.doret@chu-lyon.fr`

Abstract— **Interpretation and analysis of intrapartum fetal heart rate, enabling early detection of fetal acidosis, remains a challenging signal processing task. Recently, a variant of the wavelet-based multifractal analysis, based on *p*-exponents and *p*-leaders, which provides a rich framework for data regularity analysis, has been proposed. The present contribution aims at studying the benefits of using the *p*-leader multifractal formalism for discrimination of intrapartum fetal heart rate. First, a dependence on *p* of the multifractal properties of data is evidenced and interpreted. Second, classification between healthy subjects and fetuses suffering from acidosis is shown to have satisfactory performance that increases when *p* is decreased.**

Keywords— **wavelets, multifractal analysis, *p*-leaders, intrapartum, fetal heart rate variability, acidosis detection.**

I   INTRODUCTION

Fetal monitoring.   Fetal monitoring is commonly performed using cardiotocography, the simultaneous recording of fetal heart rate (FHR) and uterine contractions. FHR monitoring helps clinicians to identify and extract fetuses at risk before asphyxia and severe long term consequences, such as neuro-development disability, neonatal encephalopathy, and cerebral palsy, occur. Continuous FHR offers valuable information about fetal oxygenation status, and provides insight into defense mechanisms fetuses use to adapt to hypoxia. Fetuses's reactions to hypoxic events result in a complex behaviour governed by multiple nervous feedback loops and exhibiting complex FHR dynamics. In clinical practice such dynamics are captured by the measurement of short/long term variability and shifts in baseline fetal heart rate [1].

Multifractal analysis of FHR – related works.   Multifractal analysis is a recent signal processing technique that is well suited to measure information encoded in the regularity fluctuations of data. Therefore, it can be used as a natural and improved substitute of the time variability analysis classically performed on heart rate variability. It has been widely used for the analysis of adult heart rate [2–4]. It has also been used for the analysis of FHR in e.g. [5]. Multifractal analysis is based on a measure of pointwise regularity, which has traditionally been the Hölder exponent h (cf. e.g. [6] for its definition). Rather than focusing on the value that the Hölder exponent takes on each time instant, multifractal analysis provides a global description of the distribution of Hölder exponents throughout the data, the *multifractal spectrum* $D(h)$. Its practical estimation is tied to the use of specifically tailored multi-resolution quantities in a *multifractal formalism* [6].

Recently, a new measure of pointwise regularity has been introduced: the *p*-exponent [7, 8]. The corresponding multifractal formalism relies on the use of a new multiresolution quantity, the *p*-leaders [8]. The use of *p*-exponents provides a number of benefits over the Hölder exponent. First, it can take on negative values and therefore is well suited to measure *negative regularity*, which is typically present in heart rate data. Second, the dependence on parameter *p* can be used to obtain information on the presence of different kinds of *oscillatory singularities* in data [8], and hence enriches the multifractal description of singularities. Finally, estimations based on *p*-leaders have better statistical performance than Hölder exponent based ones [8, 9].

Goals, contributions and outline.   In this contribution, we conduct a study of the benefits of using a *p*-leader based multifractal formalism for discrimination of FHR of healthy fetuses against fetuses suffering from acidosis. To that end, the *p*-leader formalism (cf. Sec. III) is applied to almost 1000 FHR time series, recorded in a French academic hospital (cf. Sec. II). The aims of the study are twofold: first, to determine whether estimations change for different *p*-exponents or not; second, to assess whether the increased estimation performance for the *p*-leader multifractal formalism, shown in [9], reflects in increased discriminatory power between healthy subjects and those suffering from acidosis (cf. Sec. IV).

II   DATABASE

Database.   The database of FHR signals was collected at the public academic French Hospital Femme-Mère-Enfant in Bron, between 2000 and 2010. In total the database consists

of 3049 intrapartum cardiotocogram (CTG) signals – all acquired using a scalp electrode system STAN S21 or S31, with 12 bit resolution, 500 Hz sampling frequency (STAN, Neoventa Medical, Moelndal, Sweden). Clinical information for women and neonates were systematically collected by obstetricians in charge, cf., [10] for details.

Dilation Stage. In normal delivery, two stages of labour are recognized: the dilation stage and the active pushing stage. Studies describing the different nature of FHR during labour exist [11] but the manifestation of temporal dynamics with respect to both stages still remains unclear. Because of better signal quality, it is chosen here to perform the analysis on the last 20 minutes of the dilation stage of labour. It is required further that the last FHR measurement is taken as close in time as possible to the measurement of umbilical artery pH once labour is concluded; hence only those records with active pushing stage shorter than 10 minutes were selected. The application of such criteria leads to 905 records available for analysis, amongst which 31 fetuses were defined as having neonatal acidosis (umbilical artery pH ≤ 7.05). Hereafter, we refer to this latter group as *nonhealthy*, as opposed to *healthy*.

Preprocessing. FHR data are irregularly sampled, with $\{t_i, i = 1, \ldots, N\}$, where t_i represents the time interval between consecutive R peaks. Classically, in heart rate variability analysis, beat to beat time series are interpolated and resampled into regularly sampled signals. Since FHR does not contain frequencies beyond 3 Hz, it is chosen here to resample the FHR to 10 Hz using cubic splines interpolation.

III   METHODOLOGY

p-regularity. Multifractal analysis has been traditionally based on the use of the Hölder exponent h to measure local regularity (cf. [6] for definition). This choice imposes the restriction that only positive regularity can be measured, or, conversely, that the function under analysis must be locally bounded: $X \in L_{loc}^{\infty}(\mathbb{R})$. To overcome this restriction, it has recently been proposed to replace the Hölder exponent by the p-exponent [8]. Let $X \in L_{loc}^{p}(\mathbb{R})$ for $p \geq 1$. X is said to belong to $T_{\alpha}^{p}(t)$, with $\alpha > -1/p$, if there exist $C, R > 0$ and a polynomial P_t (with $deg(P_t) \leq \alpha$) such that $\forall \alpha < R$,

$$\left(\frac{1}{a} \int_{t-a/2}^{t+a/2} |X(u) - P_t(u-t)|^p \, du \right)^{1/r} \leq C a^{\alpha}. \quad (1)$$

The p-exponent of X at t is defined as $h_p(t) = \sup\{\alpha : X \in T_{\alpha}^{p}(t)\}$ and is a natural substitute for the Hölder exponent when dealing with functions which are not bounded but rather belong locally to L^p, and admits negative local regularity exponents $h_p > -1/p$. Obviously, the Hölder exponent equals the p-exponent for $p = \infty$; furthermore, $h_{p'} \geq h_p$ if $p' \geq p$ [8,9].

Multifractal p-spectrum. Mimicking the definition of the multifractal spectrum $D(h)$ for the Hölder exponent [6,8], the multifractal p-spectrum $D_p(h_p)$ can be defined as the Haussdorf dimension of the set of points where the p-exponent takes the value h_p. In practice, $D_p(h_p)$ can not be computed using this definition, but rather using an alternative formulation, termed *multifractal formalism*, based on p-leaders.

p-leaders. The practical estimation of the Hölder-exponent-based multifractal spectrum relies on the use of wavelet leaders [12]. Equivalently, the estimation of a p-exponent based spectrum calls for the use of p-leaders, defined as follows. Let $d_X(j,k)$ be the L^1 normalized discrete wavelet transform coefficients of X [12, 13]. Let us define the dyadic intervals $\lambda = \lambda_{j,k} = [k2^j, (k+1)2^j)$, and $3\lambda = \bigcup_{m \in \{-1,0,1\}} \lambda_{j,k+m}$. Therefore, the wavelet coefficients can be indexed as $d_\lambda = d_X(j,k)$. Then, the p-leaders are defined as [7–9]:

$$L^{(p)}(j,k) \equiv L_\lambda^{(p)} = \left(\sum_{\lambda' \subset 3\lambda} |d_{\lambda'}|^p \, 2^{-(j-j')} \right)^{1/p}. \quad (2)$$

p-leaders permit to measure p-exponent local regularity in the sense that

$$\text{for } t = 2^j k, \; L^{(p)}(j,k) \sim C 2^{j h_p(t)}, \; 2^j \to 0. \quad (3)$$

Furthermore, the definition of p-leaders enables to extend the definition of p-exponents to $0 < p < 1$, see [8] for details.

Multifractal formalism. The p-leader multifractal formalism allows to compute $D_p(h_p)$ in a practically feasible way. First, the scaling exponents $\zeta_p(q)$ are defined by the scaling behavior of the structure functions $S_p(q,j)$:

$$S_p(q,j) = 1/n_j \sum_{k=1}^{n_j} L^{(p)}(j,k)^q \sim C_{q,p} 2^{j\zeta_p(q)}, 2^j \to 0. \quad (4)$$

An (upper bound) estimate of the multifractal spectrum can be obtained as a Legendre Transform of $\zeta_p(q)$ [6]: $D_p(h_p) \leq \min_q (1 + q h_p - \zeta_p(q))$. In practice, the equality is assumed to be satisfied and the multifractal formalism is said to hold.

Log-cumulants. In real-world applications, it is useful to approximate the multifractal spectrum by a parabolic expansion: $D(h) = 1 + (h - c_1)^2 / (2c_2)$ [12]. It can be shown [8, 12] that the coefficients c_m are directly related to the scale dependence of the m-th order cumulants, $C_m^{(p)}(j)$, of $\ln L^{(p)}(j, \cdot)$:

$$C_m^{(p)} = \text{Cum}_m \ln L^{(p)}(j, \cdot) = c_m^{(0,p)} + c_m^{(p)} \ln 2^j + \gamma(j,p), \quad (5)$$

where $\gamma(j,p)$ is a nonlinear function whose precise expression is given in [8]. Eq. (5) is used for practical estimation of the $c_m^{(p)}$ by linear regression of the estimates of $C_m^{(p)}(j)$ against $\ln 2^j$, for $j \in [j_1, j_2]$. The estimation procedures, implemented by ourselves in the MATLAB programming language, are used to obtain the results in Sec. IV.

Pseudo-fractional integration. In practice, it must be verified that $X \in L^p(\mathbb{R})$ before computing p-leaders. This
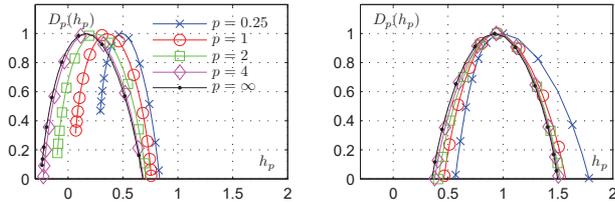
Fig. 1: **Dependence on p:** estimated multifractal spectra for typical healthy (left) and nonhealthy (right) subjects.

Fig. 2: **Dependence on p:** mean of the estimations of c_1 (left) and c_2 (right), with 95% confidence intervals.

Table 1: **Dependence on p:** p-values for Kruskal-Wallis tests with $H_0 : c_m^{(p)} = c_m^{(p')}$ for $m = 1, 2$, and for healthy and nonhealthy groups.

	c_1	c_2
HEALTHY	$1.70e-22$	$2.13e-133$
NONHEALTHY	0.83	0.03

can be easily done by checking the condition: $\eta(p) = 1/n_j \sum_{k=1}^{n_j} |d_X(j,k)|^p \geq 0$ [7, 8]. If the condition is found not to hold, a pseudo fractional integration in the wavelet domain can be performed [12]. It must be chosen such that $\eta^{(-\gamma)}(p) = \eta(p) + \gamma p \geq 0$, where $^{(-\gamma)}$ indicates that a quantity was computed from a pseudo-fractional integral $X^{(-\gamma)}$ of order γ of X. The pseudo fractional integration is performed by computing the wavelet p-leaders of the modified wavelet coefficients $d_X^{(-\gamma)}(j,k) = 2^{-\gamma j} d_X(j,k)$ [8, 12].

IV   RESULTS AND DISCUSSION

Experimental setup.   Wavelet coefficients were computed using a Daubechies mother wavelet with $N_\psi = 3$ vanishing moments. Estimations were performed using $p \in \{0.25, 0.5, 1, 2, 4, 10, \infty\}$ and a scaling range $j_1 = 6$, $j_2 = 10$. The minimum regularity condition $\eta(p) > 0$ was checked a priori for all subjects, and it was determined that a fractional integration of order $\gamma = 0.5$ was needed. Data processing and statistical analysis was performed in MATLAB.

Fetal heart rate and multifractal attributes.   Fig. 1 displays estimated spectra for $p \in \{0.25, 1, 2, 4, \infty\}$, for a representative healthy (left) and nonhealthy (right) subjects. It shows that, whatever p, spectra for the nonhealthy subjects are to the right of those for healthy ones. Fig. 2 displays the average of the estimates of c_1 (left) and c_2 (right), with 95% confidence intervals, for healthy (black lines) and nonhealthy (red lines) subjects, and shows that healthy subjects have smaller c_1 and larger $|c_2|$ than nonhealthy ones, for all p. The large difference in the widths of the confidence intervals between healthy and nonhealthy subjects stems from the unbalanced sizes of the classes (874 healthy and 31 nonhealthy records). Figs. 1 and 2 thus both indicate that FHR time series for nonhealthy subject are characterized by more regularity as measured by multifractal analysis: Larger c_1 and smaller $|c_2|$, and thus by a decrease of heart rate variability. This suggests that multifractal analysis can potentially be used for early acidosis detection.

Fetal heart rate and dependence on p.   Fig. 1 also suggests that as p decreases from ∞ (black line) to 0.25 (blue line), p-spectra are shifted to larges values of h and become more narrow. In addition, Fig. 2 shows that estimations of
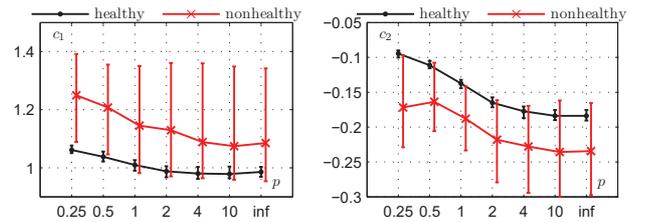
c_1 and c_2 for both groups indeed display dependence on p. To assess whether differences c_1 and c_2 for different p are significant or not, for both groups, Kruskal-Wallis tests are performed. Results, reported in Table 1, show that the null hypothesis (no difference between estimations for different p) is strongly rejected for the healthy group, with a very low p-value. To the contrary, the test rejects the null hypothesis at a 5% confidence level for c_2 for the unhealthy group, but fails to do so for c_1. Dependence on p is thus clear, obvious and significant for the healthy group. Dependence on p remains slightly less easy to assess for the nonhealthy group, likely due to its significantly smaller sample size yielding thus a reduced power of the test.

As discussed in [8], the fact that p-spectra vary with p has a profound and deep meaning: It provides evidence that data have a special sort of oscillating singularities called *lacunary singularities*, and not only consist of simpler canonical singularities, referred to as cusps [8]. Therefore, Figs. 1 and 2, as well as Table 1, showing a significant dependence on p, indicate that healthy FHR are characterized by a rich oscillatory singularity behavior with potentially lacunary singularities. This broadens the description provided up to now by Hölder exponent based analysis, by permitting to distinguish lacunary singularities from the canonical ones. Further, Fig. 2 and Table 1 also suggest that the dependence on p for nonhealthy FHR is less significant. If confirmed, this would mean that complex oscillatory behaviors existing in healthy FHR temporal dynamics are decreased under acidosis.

Discrimination between healthy and nonhealthy subjects. To study the impact of p on classification performance, c_1 and c_2 are computed for all subjects. Receiver operator characteristic (ROC) curves are computed independently for c_1 and c_2, and the area under ROC curve (AUC) are computed. Results in Table 2 and Fig. 3 clearly show that lower values of p achieve better classification performance. For larger values

Table 2: **Classification performance.** AUC values for different p.

	0.25	0.5	1	2	4	10	∞
c_1	0.71	0.70	0.69	0.67	0.67	0.67	0.67
c_2	0.66	0.63	0.62	0.61	0.60	0.60	0.60
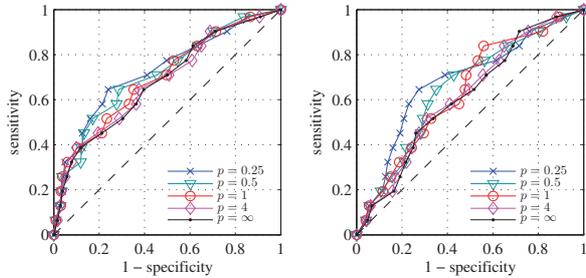
Fig. 3: ROC curves for c_1 (left) and c_2 (right), for several values of p.

Fig. 4: **Joint use of c_1 and c_2 for $p = 0.25$.** Left: Fisher linear discriminant analysis of c_1 and c_2; points with $c_2 < -0.35$ are plotted as $c_2 = -0.35$ for better readability of the main clusters. Right: ROC curve for c_1, c_2 and FLD jointly c_1 and c_2.

of p, AUC decreases markedly. Notably for $p = \infty$, estimates of c_2 are less reliable showing large variance, and thus classification performance are lower compared to those obtained with $p = 0.25$. The difference between AUC for c_1 and c_2 is mainly due to performance in the lower part of ROC curves (better sensitivity and specificity in left bottom corner for c_1).

Further, Fisher Linear Discriminant (FLD) analysis is applied to (c_1, c_2), for $p = 0.25$, to explore the benefits of the joint use of c_1 and c_2. The use of five fold cross validation technique induces a slight improvement in performance, with AUC reaching 0.73 ± 0.09. Fig. 4 depicts linear separation of healthy (left side from separating line) and nonhealthy (right side) domains. First, on the lower right side, the higher density of nonhealthy cases highlights that c_1 and c_2 well characterize FHR regularity of fetuses with acidosis. Second, on the upper left side, there remain a number of nonhealthy subjects in the healthy domain. Preliminary analysis of such subjects indicates that the dependence on p of multifractal attributes, as described in Fig. 1, resembles that observed for healthy subjects. The reason for this is under current investigation.

V   CONCLUSIONS

This contribution illustrates the benefits provided by the p-leader formalism for the characterization and discrimination of intrapartum FHR data. First, non healthy subjects mostly show an increased regularity, and thus less variability in FHR temporal dynamics. Second, a significant dependence on p for healthy FHR is observed, which can be interpreted as the fact that FHR temporal dynamics involve complex singular behaviors (reminiscent of lacunary singularities). Moreover, dependence on p for nonhealthy FHR is potentially weaker, again pleading for decreased variability. This seems to also be
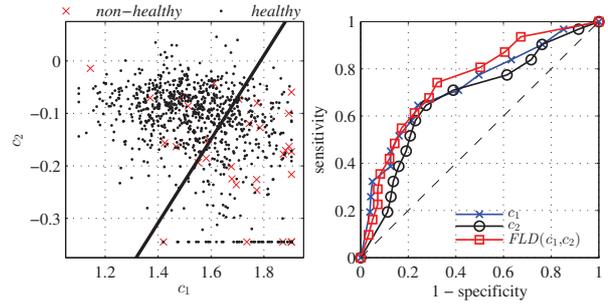
the case for subjects affected by acidosis. In addition, classification performance between healthy and nonhealthy FHR was shown to improve, with respect to the traditional wavelet leaders, with the use of this novel technique and small p which may stem from two reasons: p-leader multifractal formalism provides richer information by considering the oscillatory behavior; p-leaders provide better estimation performance for small values of p.

REFERENCES

1. FIGO. Guidelines for the Use of Fetal Monitoring *International Journal of Gynecology & Obstetrics.* 1986;25:159-167.
2. Ivanov P. Ch. et al. Multifractality in human heartbeat dynamics *Nature.* 1999;399:461-465.
3. Kiyono K. et al. Multiscale probability density function analysis: non-Gaussian and scale-Invariant fluctuations of healthy human heart rate *IEEE Trans. Biomed. Eng..* 2006;53:95-102.
4. Leonarduzzi R., Schlotthauer G., Torres M. E.. Wavelet leader based multifractal analysis of heart rate variability during myocardial ischaemia in *Conf Proc IEEE Eng Med Biol Soc*:110 -113 2010.
5. Doret M. et al. Multifractal analysis of fetal heart rate variability in fetuses with and without severe acidosis during labor *American journal of perinatology.* 2011;28:259.
6. Riedi R.H.. Multifractal Processes in *Theory and applications of long range dependence* (Doukhan P., Oppenheim G., Taqqu M.S.. , eds.):625-717Birkhäuser 2003.
7. Jaffard S., Melot C.. Wavelet analysis of fractal boundaries *Communications In Mathematical Physics.* 2005;258:513–565.
8. Jaffard S. et al. p-Exponent and p-Leaders: Negative pointwise regularity and beyond *in preparation.* 2014.
9. Leonarduzzi R. et al. Extending multifractal analysis to negative regularity: p-exponents and p-leaders in *IEEE Int. Conf. Acoust., Speech, and Signal Proc. (ICASSP)*(Florence, Italy) May 2014. to appear.
10. Doret M. et al. Use of peripartum ST analysis of fetal electrocardiogram without blood sampling: a large prospective cohort study. *Eur J Obstet Gynecol Reprod Biol.* 2011;156:35–40.
11. Gonçalves P. et al. Linear and nonlinear fetal heart rate analysis of normal and acidemic fetuses in the minutes preceding delivery *Med Biol Eng Comput.* 2006;44:847–855.
12. Wendt H., Abry P., Jaffard S.. Bootstrap for Empirical Multifractal Analysis *IEEE Signal Proc. Mag..* 2007;24:38–48.
13. Mallat S.. *A Wavelet Tour of Signal Processing*. San Diego, CA: Academic Press 1998.